Available online at www.sciencedirect.com

SciVerse ScienceDirect

Scripta Materialia 68 (2013) 627–630

Scripta MATERIALIA

www.elsevier.com/locate/scriptamat

Size- and temperature-dependent piezoelectric properties of gallium nitride nanowires

Jin Zhang,[a] Chengyuan Wang,[a,c,*] Rajib Chowdhury[b] and Sondipon Adhikari[a]

[a]*College of Engineering, Swansea University, Singleton Park, Swansea SA2 8PP, UK*
[b]*Department of Civil Engineering, Indian Institute of Technology Roorkee, Roorkee 247667, India*
[c]*Faculty of Civil Engineering and Mechanics, Jiangsu University, 301, Xuefu Road Zhenjiang, 212013, Jiangsu PR China*

Received 25 November 2012; revised 14 December 2012; accepted 17 December 2012
Available online 23 December 2012

The piezoelectric constant e_{33} is calculated using molecular dynamic simulations for square gallium nitride (GaN) nanowires (NWs). Its magnitude is found to decrease significantly with increasing cross-section and temperature. An attempt is made to understand the physics behind the size- and temperature dependence of e_{33}. Specifically, a constant surface piezoelectric coefficient $e_{33}^{s} = 0.52 \times 10^{-9}$C/m is achieved for square GaN NWs independent of the geometric size of their cross-sections.

Keywords: Gallium nitride; Nanowire; Piezoelectricity; Molecular dynamics

Ambient sources of power, such as thermal, wind and biomechanical energy, are readily available. One advantageous approach towards harvesting energy from alternative sources is the utilization of semiconducting piezoelectric materials [1], which facilitate the conversion of mechanical energy into electrical energy. In this regard [2], the use of piezoelectric energy harvesters is emerging as an effective strategy to power wireless sensor nodes [3] and personal electronics alongside the more extensively studied thermoelectric and solar-based methods. In fact, for conditions of indoor lighting or where long operational lifetime is required, piezoelectric energy harvesting yields a greater power density (power generated per volume of the system) than other strategies where energy is also scavenged from motion. Recently this strategy has been employed on the nanoscale by using zinc oxide (ZnO) and gallium nitride (GaN) nanocrystals. These nanomaterials are achieved in various configurations, among which quasi-one-dimensional (1-D) nanowires (NWs) and nanobelts (NBs) are the most frequently synthesized and are promising materials for the structural and functional elements in various smart nanodevices and nanoelectronics [4–6]. Thus, considerable effort has been invested in characterizing the elastic [7], piezoelectric and semiconducting properties of piezoelectric NWs and NBs [8–12].

It has been noted in previous studies [13–16] that the high surface-to-volume ratio at the nanoscale could dramatically enhance the surface effect and could ultimately lead to distinct elastic and piezoelectric properties that are significantly different from their macroscopic counterparts. The elastic and piezoelectric properties have already been studied extensively for ZnO NWs [8–12]. Both experimental techniques [17–20] and simulation methods, e.g. first-principle calculations [21,22] and molecular dynamic simulations (MDS) [17,23–27], have been employed. The results show that the elastic and piezoelectric properties of the ZnO nanocrystals are size dependent. In particular, the piezoelectric constants could be up to orders of magnitude greater than their bulk counterparts. It is also observed that the material properties, e.g. the Young's modulus, of ZnO NWs vary significantly when the shapes of their cross-sections change [23,26].

Similar to ZnO, crystalline GaN is characterized by the wurtzite structure. To date, nanoscale GaN has received little attention, although it exhibits much better chemical stability than ZnO and sometimes stronger piezoelectric responses [28]. Here the chemical stability is crucial for the performance of smart nanodevices running under severe environmental conditions. Very recently, initial investigations have been carried out on the elastic [29–32] and piezoelectric [22] properties of

* Corresponding author at: College of Engineering, Swansea University, Singleton Park, Swansea SA2 8PP, UK; e-mail: chengyuan.wang@swansea.ac.uk

1359-6462/$ - see front matter © 2012 Acta Materialia Inc. Published by Elsevier Ltd. All rights reserved.
http://dx.doi.org/10.1016/j.scriptamat.2012.12.022

hexagonal GaN NWs. The piezoelectric properties of square GaN NWs, however, still remain an open topic. Specifically, the observation on ZnO NWs suggests that these properties should be significantly different from those obtained for hexagonal GaN NWs.

In this letter, the piezoelectric properties of square GaN NWs and their dependence on the size and temperature are studied based on MDS, which is more efficient than the frequently used ab initio method and thus enables us to deal with a larger computational system. Subsequently, a piezoelectric core–surface (CS) composite beam model was employed to reveal the physical origin of the size dependency of the piezoelectric properties.

In this study, we focused our attention on the most common square GaN NW [28], the growth direction of which is along the c-axis [0001], with the transverse side surfaces being $[2\bar{1}\bar{1}0]$ and $[01\bar{1}0]$ (Fig. 1). The length L of the NWs is fixed at15 nm, whereas the size b of the square cross-section varies from 1 nm to 4 nm. In the present MDS, the interactions between Ga–Ga, N–N and Ga–N were described by the Stillinger–Weber (SW) potential [33], which was employed to evaluate the elastic properties of GaN NWs in Refs. [30,31]. Its analytical form is available in the Supplementary material, where the optimized lattice parameters for the SW potential of GaN can also be found. The NVT ensemble (constant number of particles, volume and temperature) was employed to update the positions and velocities of the atoms after each time step using a Nosé–Hoover temperature thermostat [34]. At the beginning of all simulations, the equilibrium of the initialized structure was achieved, corresponding to the lowest energy of the NWs. After full relaxation, certain treatments were applied to calculate the piezoelectric properties. Here all MDS were conducted using a large-scale atomic/molecular massively parallel simulator [35] without periodic boundary conditions.

We first study the piezoelectric responses of GaN NWs. For such 1-D nanostructures, the piezoelectric property in the axial direction (c-axis) is of major concern, and can be characterized by the piezoelectric constant e_{33}, defined as [36] $e_{33} = -\partial\sigma_3/\partial E_3$. Here σ_3 and E_3 denote the stress and electric field strength along the axial direction, respectively. Before calculating e_{33}, we fixed the two ends of the NWs after the initial relaxation. The purpose of doing this was to avoid any prestrains in the structure. An electric field in the axial direction was then applied to the NWs at room temperature $T = 300$ K (see the inset of Fig. 2). The external

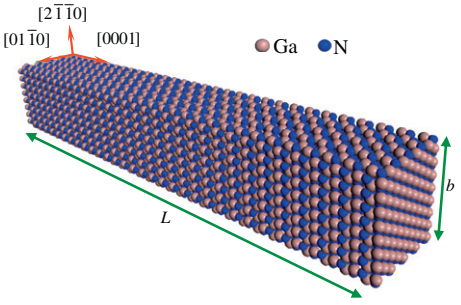

Figure 1. Molecular representation of a square GaN NW assembled in the [0001] growth orientation.

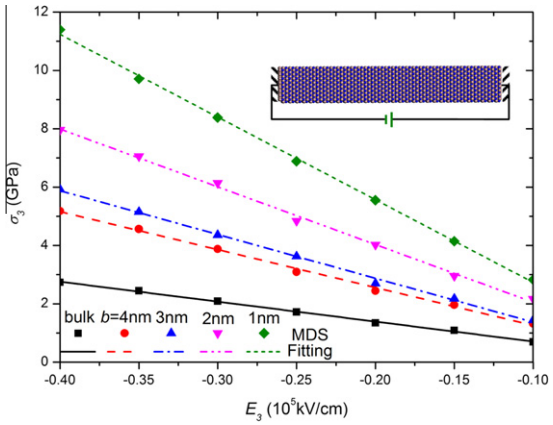

Figure 2. Stress–electric field strength curves for bulk GaN and GaN NWs with different cross-section sizes.

force on ion i due to the electric field can be expressed as $F_i = q_i E_3$, where q_i is the charge on ion i (+3e for Ga^{3+} and −3e for N^{3-}). Finally, the stress σ_3 in the axial direction was calculated by dividing the resultant force by the area of the cross-section. These results are shown in Figure 2 as a function of E_3 for NWs with different cross-sectional sizes b. Similar results are also plotted in Figure 2 for bulk GaN with a simulation cell size of $10 \times 10 \times 10$ unit cells and periodic boundary conditions along three coordinate directions. From the definition given above, the piezoelectric constant e_{33} is equal to the negative slope of the $\sigma_3 - E_3$ curves. As seen from Figure 2, σ_3 rises almost linearly with increasing electric field strength E_3. This leads to an almost constant e_{33} of GaN NWs, which, as noted in Figure 2, decreases with growing cross-sectional size b. Specifically, the value of e_{33} obtained for bulk GaN is 0.69C m^{-2}, which is very close to the 0.73C m^{-2} obtained in an ab initio study [37].

The size dependence of e_{33} obtained in Figure 2 is plotted in Figure 3, in comparison with that of square ZnO NWs achieved in an MDS study [25] and hexagonal GaN and ZnO NWs calculated based on the density functional theory (DFT) [38]. It is noted that, while square cross-sections could be measured by the thick-

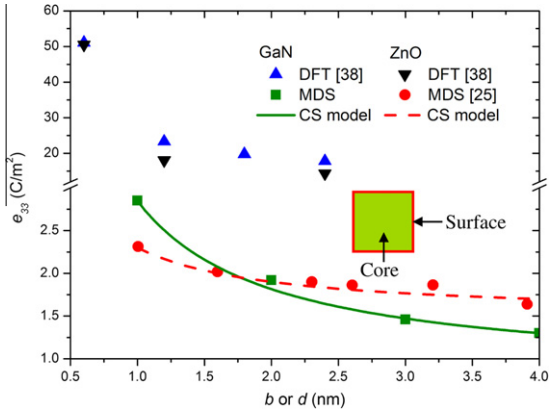

Figure 3. The piezoelectric constant of GaN and ZnO NWs as a function of the cross-section size, which were obtained based on DFT, MDS and the CS model.

ness b in the present study and Ref. [25], the hexagonal cross-sections are characterized by an effective diameter d in Ref. [38]. In Figure 3, the present MDS show that e_{33} of square GaN NWs increases by 120% as b decreases from 4 nm to 1 nm. This tendency is analogous to the size dependence of e_{33} obtained for square ZnO NWs in the MDS [25]. However, the slope of the GaN curve is always greater than that of the ZnO curve, indicating that the size effect is more pronounced for the GaN NWs. For example, although at $b = 1$ nm the e_{33} of the GaN NW is larger than that of the ZnO NW, the former is only half of the latter when b increases to 4 nm.

It can also be seen from Figure 3 that the MDS results for square GaN and ZnO NWs are qualitatively similar to the DFT results for hexagonal GaN and ZnO [38]. However, the MDS predicts values of e_{33} that are much smaller than those given by the DFT [38]. The discrepancy between MDS and DFT was also observed for nanofilms in Ref. [39]. Indeed, further study needs to be conducted to examine the accuracy of these techniques based on experimental data and provide a theoretical explanation for the discrepancy in their numerical calculations. Another factor that could contribute to the discrepancy is the shapes of the cross-sections considered, i.e. square or hexagonal. This is because, even for the same nanocrystalline material, the different shape of the cross-section suggests that the growth direction and the corresponding facets could be different for the nanostructures considered. In addition, the surface-to-volume ratio may also change due to the variation of the shape of cross-section. This could exert a significant influence on the surface effect, which, as will be shown below, plays a key role in determining the overall piezoelectric properties of nanomaterials.

To understand the observed size dependence of the piezoelectric constant, a widely accepted CS model was employed, in which an NW is modelled as a composite beam consisting of the core section of the bulk material and the surface layers (inset of Fig. 3). The CS model was first employed to explain the size-dependent elastic properties and mechanical behaviour of nanostructures [17,19,20,40–42], and was later extended by Huang and Yu [43] to evaluate the surface effect on the piezoelectric responses of nanostructures. In this refined CS model, a piezoelectric surface was introduced with a piezoelectric constant that could be calculated by fitting the CS model to MDS [39]. Based on the CS model, the effective piezoelectric constant of NWs is calculated by [39] $e_{33} = e_{33}^b + 4e_{33}^s/b$ (square NWs), where e_{33}^b is the bulk piezoelectric constant and e_{33}^s is the surface piezoelectric constant. In Figure 3 the CS model with properly selected values of e_{33}^b and e_{33}^b is found to be in excellent agreement with the MDS in predicting the e_{33} of square GaN and ZnO NWs. For the core section, the e_{33}^b used in the CS model is 0.76C m^{-2} for GaN NWs, which is in accordance with both the 0.69C m^{-2} obtained in the present MDS and the 0.73C m^{-2} given by the ab initio study [37]. In addition, $e_{33}^b = 1.5\text{C/m}^2$ for ZnO NWs is also close to the 1.4C m^{-2} predicted by the MDS [25]. For the surface layers, $e_{33}^s = 0.52 \times 10^{-9}$C/m is obtained for the GaN NWs, which is greater than the $e_{33}^s = 0.2 \times 10^{-9}$C/m used for the ZnO NWs in the CS model.

GaN is also a pyroelectric crystal, the polarization of which strongly depends on its environmental temperature. It is thus of interest to examine the thermal effect on the piezoelectric properties of GaN NWs, which is also related to the polarization of the crystal. Conceptually, temperature reflects the kinetic energy of atoms. At non-zero temperatures, the atoms of GaN crystals vibrate due to thermal oscillations around their equilibrium positions. MDS is considered to be a valuable tool for investigating such dynamical processes at non-zero temperatures.

Following the procedure demonstrated previously (see Page 2), we measured the piezoelectric constant e_{33} of GaN NWs at different temperatures. Figure 4 shows the results obtained for GaN NWs of various thicknesses and bulk GaN at a temperature T rising from 100 to 500 K. It can be seen from Figure 4 that the epiezoelectric effect of the GaN NWs and bulk GaN is sensitive to temperature change, i.e. it decreases significantly as the temperature increases. For example, T rising from 100 to 500 K leads to a decrease in e_{33} of about 20% for NWs with $b = 2$ nm and approximately 16% for the bulk GaN crystal. In other words, the piezoelectric effect becomes less significant at higher temperature for both GaN nanocrystal and bulk GaN. This tendency is also found in bulk ZnO [44]. It is thus reasonable to expect that, when the temperature rises to a critical value, the e_{33} of GaN NWs would tend to zero. It is well known that for bulk piezoelectric materials the polarization generally decreases as the environmental temperature increases. Specifically, when the temperature increases to the so-called Curie temperature, their polarization is lost [45]. Thus the thermal effect on piezoelectricity predicted by the present MDS for GaN NWs is significant and reasonable, and therefore should be taken into consideration in designing piezoelectronics and other smart nanodevices operating in a wide temperature range.

In summary, molecular dynamics simulations were performed to study the piezoelectric properties of square GaN NWs and bulk GaN crystal. The piezoelectric constant e_{33} of the GaN NWs is found to increase with

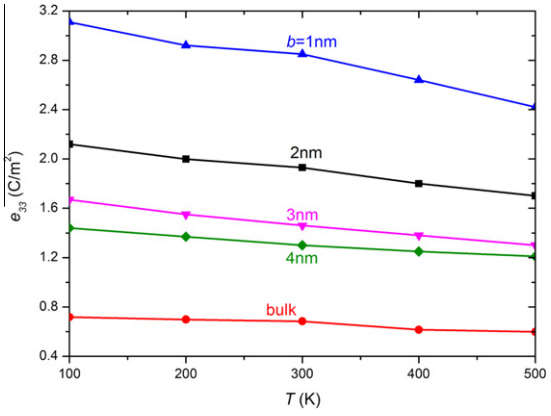

Figure 4. The piezoelectric constant of the bulk GaN and the GaN NWs as a function of temperature.

decreasing cross-sectional size and is greater than the corresponding bulk value. The size dependence of the piezoelectric constant is observed, and is explained well in terms of surface piezoelectricity using a core–surface composite beam model. The values of surface piezoelectricity were obtained, which could then be employed in the theoretical analysis based on equivalent continuum mechanics theory. Finally, it is demonstrated that the piezoelectric constants of the GaN NWs and bulk GaN decrease with increasing temperature as a result of the temperature dependence of material polarization. These results obtained based on MDS could provide important guidance in the design, fabrication and application of GaN NW-based optoelectronic and electronic devices.

J.Z. acknowledges the support from the China Scholarship Council (CSC). S.A. acknowledges the support from the Royal Society through the award of Wolfson Research Merit Award.

Supplementary data associated with this article can be found, in the online version, at http://dx.doi.org/10.1016/j.scriptamat.2012.12.022.

[1] Y. Zhang, Y. Liu, Z.L. Wang, Adv. Mater. 23 (2011) 3004.
[2] Z.L. Wang, J.H. Song, Science 312 (2006) 242.
[3] G. Litak, M.I. Friswell, S. Adhikari, Appl. Phys. Lett. 96 (2010) 214103.
[4] Y. Qin, X.D. Wang, Z.L. Wang, Nature 451 (2008) 809.
[5] C.Y. Chen, G. Zhu, Y.F. Hu, J.W. Yu, J.H. Song, K.Y. Cheng, L.H. Peng, L.J. Chou, Z.L. Wang, ACS Nano 6 (2012) 5687.
[6] C.S. Lao, Q. Kuang, Z.L. Wang, M.C. Park, Y.L. Deng, Appl. Phys. Lett. 90 (2007) 262107.
[7] R. Chowdhury, S. Adhikari, F. Scarpa, Physica E 42 (8) (2010) 2036.
[8] S. Xu, Y. Qin, C. Xu, Y. Wei, R.U. Yang, Z. Wang, Nat. Nanotechnol. 5 (2010) 366.
[9] Y. Ding, Z.L. Wang, Micron 40 (2009) 3.
[10] X.D. Bai, P.X. Gao, Z.L. Wang, E.G. Wang, Appl. Phys. Lett. 82 (2003) 26.
[11] Y.H. Huang, X.D. Bai, Y. Zhang, J. Phys.: Condens. Matter 18 (2006) L179.
[12] H. Ni, X.D. Li, Nanotechnology 17 (2006) 3591.
[13] H.S. Park, P.A. Klein, J. Mech. Phys. Solids 56 (2008) 3144.
[14] R. Dingreville, J.M. Qu, M. Cherkaoui, J. Mech. Phys. Solids 53 (2005) 1827.
[15] P.A.T. Olsson, H.S. Park, J. Mech. Phys. Solids 60 (2012) 2064.
[16] R.C. Cammarata, Mat. Sci. Eng. A 237 (1997) 180.
[17] C.Q. Chen, Y. Shi, Y.S. Zhang, J. Zhu, Y.J. Yan, Phys. Rev. Lett. 96 (2006) 075505.
[18] R. Agrawal, B. Peng, E.E. Gdoutos, H.D. Espinosa, Nano Lett. 2008 (8) (2008) 3668.
[19] F. Xu, Q. Qin, A. Mishra, Y. Gu, Y. Zhu, Nano Res. 3 (2010) 271.
[20] A. Asthana, K. Momeni, A. Prasad, Y.K. Yap, R.S. Yassar, Nanotechnology 22 (2011) 265712.
[21] H.J. Xiang, J.L. Yang, J.G. Hou, Q.S. Zhu, Appl. Phys. Lett. 89 (2006) 223111.
[22] R. Agrawal, H.D. Espinosa, Nano Lett. 11 (2011) 786.
[23] A.J. Kulkarni, M. Zhou, F.J. Ke, Nanotechnology 16 (2005) 2749.
[24] S.X. Dai, M.L. Dunn, H.S. Park, Nanotechnology 21 (2010) 445707.
[25] K. Momeni, G.M. Odegard, R.S. Yassar, Acta Mater. 60 (2012) 5117.
[26] J. Hu, X.W. Liu, B.C. Pan, Nanotechnology 19 (2008) 285710.
[27] S.X. Dai, H.S. Park, J. Mech. Phys. Solids 61 (2013) 385.
[28] R.M. Yu, L. Dong, C.F. Pan, S.M. Niu, H.F. Liu, W. Liu, S.J. Chua, D.Z. Chi, Z.L. Wang, Adv. Mater. 24 (2012) 3532.
[29] C.Y. Nam, P. Jaroenapibal, D. Tham, D.E. Luzzi, S. Evoy, J.E. Fischer, Nano Lett. 6 (2006) 153.
[30] R.A. Bernal, R. Agrawal, B. Peng, K.A. Bertness, N.A. Sanford, A.V. Davydov, H.D. Espinosa, Nano Lett. 11 (2011) 548.
[31] Z.G. Wang, X.T. Zu, L. Yang, F. Gao, W.J. Weber, Phys. Rev. B 76 (2007) 045310.
[32] A. Gulans, I. Tale, Phys. Status Solidi C 4 (2007) 1197.
[33] F.H. Stillinger, T.A. Weber, Phys. Rev. B 31 (1985) 5262.
[34] S. Nosé, J. Chem. Phys. 81 (1984) 511.
[35] S.J. Plimpton, J. Comput. Phys. 117 (1995) 1.
[36] V.V. Kochervinskii, Crystallogr. Rep. 48 (2003) 649.
[37] F. Bernardini, V. Fiorentini, Phys. Rev. B 56 (1997) R10024.
[38] M. Minary-Jolandan, R.A. Bernal, I. Kuljanishvili, V. Parpoil, H.D. Espinosa, Nano Lett. 12 (2012) 970.
[39] S.X. Dai, M. Gharbi, P. Sharma, H.S. Park, J. Appl. Phys. 110 (2011) 104305.
[40] X.P. Zheng, Y.P. Cao, B. Li, X.Q. Feng, G.F. Wang, Nanotechnology 21 (2010) 205702.
[41] R.E. Miller, V.B. Shenoy, Nanotechnology 11 (2000) 139.
[42] J. Zhang, C.Y. Wang, R. Chowdhury, S. Adhikari, Appl. Phys. Lett. 101 (2012) 093109.
[43] G.Y. Huang, S.W. Yu, Phys. Status Solidi B 243 (2006) R22.
[44] N.A. Hill, U. Waghmare, Phys. Rev. B 62 (2000) 8802.
[45] J.W. Hong, D.N. Fang, Appl. Phys. Lett. 92 (2008) 012906.